

RESEARCH

Open Access



Two 3' proximal hairpins play a key role in the replication of wheat yellow mosaic virus

Guowei Geng^{1,2*} , Minjun Liu^{2,3} and Xuefeng Yuan^{2*}

Abstract

Wheat yellow mosaic virus (WYMV), a member of the genus *Bymovirus*, causes substantial losses in wheat production in East Asia, including China and Japan. Although genomic RNA replication is an important process in the viral life cycle, the independent regulation of WYMV RNA replication by its 3' and 5' untranslated regions (UTRs) remains unclear. In this study, we sought to analyze the core structural features of the 3' UTR in the regulation of the replication of WYMV RNA1 in vitro, locate the viral RNA sites to which the NIb protein binds, and determine the regulatory effects of the VPg, P3, and 14 K proteins on NIb RNA-dependent RNA polymerase (RdRp) activity. We found that the NIb protein in WYMV RNA1 only specifically recognized its 3' UTR as the core enzyme for replication. Moreover, the 14 K and P3 proteins were established to synergistically enhance the in vitro RdRp activity of the NIb protein, whereas the VPg protein was found to play an inhibitory role. Based on RNA structure probing and mutational analysis, we identified ⁷⁶²⁴UU and ⁷⁵⁷¹UU as putative sites for interaction with the NIb protein and demonstrated that replication is dependent on their coexistence. In addition, hairpins 2 and 5 of the 3' UTR were found to be essential for NIb protein replication. Collectively, the findings of our in vitro analysis of the replication regulatory elements of WYMV RNA1 3' UTR, provide a basis for in vivo studies on the regulation of WYMV replication and the identification of potential targets for the prevention and control of WYMV-caused crop diseases.

Keywords Replication regulation, NIb, In vitro replication, Wheat yellow mosaic virus

Background

Most plant RNA viruses comprise a single-stranded genome, and once having invaded host cells, these viruses undergo protein translation, genome replication and packaging, and movement to complete their life cycle. RNA viral genome replication is an important

process in the viral life cycle and requires the participation of replication enzymes. The main component among these replication enzymes is the virus-encoded RNA-dependent RNA polymerase (RdRp), which also requires the involvement of auxiliary proteins and host factors (Koonin et al. 1989; Lewandowski and Dawson 2000; Ferrer-Orta et al. 2006). There are two main mechanisms underlying the initiation of replication, namely, primer-dependent and primer-independent processes (van Dijk et al. 2004). Viral genome replication essentially entails the synthesis of complementary negative-sense RNA by a virus-encoded replication enzyme using positive-sense RNA as a template, followed by the synthesis of new positive-sense RNA using the negative-sense RNA as a template to complete viral RNA replication.

The regulation of RNA virus replication is mediated by a core regulatory element at the 3' end of the genome that determines the initiation of replication. The structural

*Correspondence:

Guowei Geng
guowgeng@163.com
Xuefeng Yuan
snowpeak77@163.com

¹The Engineering Research Institute of Agriculture and Forestry, Ludong University, Yan'tai 264025, China

²Department of Plant Pathology, College of Plant Protection, Shandong Agricultural University, Shandong Province Key Laboratory of Agricultural Microbiology, Tai'an 271018, China

³Muping Agricultural Technology Service and Extension Center, Yan'tai 264100, China



© The Author(s) 2025. **Open Access** This article is licensed under a Creative Commons Attribution 4.0 International License, which permits use, sharing, adaptation, distribution and reproduction in any medium or format, as long as you give appropriate credit to the original author(s) and the source, provide a link to the Creative Commons licence, and indicate if changes were made. The images or other third party material in this article are included in the article's Creative Commons licence, unless indicated otherwise in a credit line to the material. If material is not included in the article's Creative Commons licence and your intended use is not permitted by statutory regulation or exceeds the permitted use, you will need to obtain permission directly from the copyright holder. To view a copy of this licence, visit <http://creativecommons.org/licenses/by/4.0/>.

characteristics of these regulatory elements are diverse, with some having complex secondary or tertiary structures, whereas others have short sequences without obvious high-level structures (Dreher 1999; Turner and Buck 1999). In addition to these core regulatory elements, there are other sequences and structural features in the 3' region that play roles in enhancing or attenuating the regulation of replication (Kim and Makino 1995; Pogany et al. 2003; Zhang et al. 2004). The 5' end sequence of RNA also participates in the regulation of replication, completing RNA cyclization via long-distance RNA-RNA interactions with the 3' end, thereby enhancing the efficiency of replication (Kim and Hemenway 1999; Khromykh et al. 2001; Miller and White 2006; Sanford et al. 2019). In addition, the 3' terminal region of the genome alters its corresponding structure via interactions with the RdRp, thereby enabling certain RNA viruses to complete the conversion between translation and replication (Yuan et al. 2009).

Wheat yellow mosaic virus (WYMV, *Bymovirus triticitessellati*), a member of the genus *Bymovirus* in the family of *Potyviridae*, causes substantial losses in wheat production in East Asia, including China and Japan (Namba et al. 1998; Chen et al. 1999; Yu et al. 1999; Wang et al. 2010). Its symptoms are similar to diseased wheat caused by filamentous viruses transmitted by *Polymyxa graminis* in Europe, Asia, and North America, such as Soilborne wheat mosaic virus (Lin and Ruan 1986; Hariri et al. 1987). The genome of WYMV is comprised of two positive single-stranded RNAs, with a covalently bound VPg protein at the 5' end and a poly (A) tail at the 3' end. Both RNA1 and RNA2 encode polyproteins that can be cleaved by virus-encoded proteinases to yield 10 mature viral proteins (Namba et al. 1998; Li et al. 1999; Li and Shirako 2015). Nucleotide sequences of the coding regions and 3' UTR of different WYMV isolates are generally characterized by high identities, whereas the 5' UTR tends to have a relatively higher rate of mutation (Geng et al. 2017). Moreover, compared with the 5' UTR of WYMV RNA2, that of WYMV RNA1 has a higher homology among different WYMV isolates (Geng et al. 2017). However, recent studies have found that the 3' end of WYMV lacks adenylation, and 3' polyadenylation has negative effects on the synthesis of the minus-strand of WYMV RNA in vitro (Geng et al. 2019a). Furthermore, IRES elements have been identified in the 5' UTR of WYMV RNA1 and RNA2, which can regulate the cap-independent translation of WYMV. However, whereas the 3' UTR can synergistically enhance the IRES activity of the corresponding 5' UTR (Geng et al. 2020, 2024). However, the independent regulation of replication by 3' UTR and 5' UTR in this virus has yet to be sufficiently determined.

A number of the proteins encoded by the WYMV have been speculated to be associated with WYMV replication based on their functions. Nib has RNA-dependent RNA polymerase activity and is assumed to be the core protein involved in viral replication (Geng et al. 2019b). Studies have shown that by interacting with the light-induced protein LIP, Nib can interfere with the ABA pathway, thereby promoting WYMV infection (Zhang et al. 2019a, b). In picornaviruses, VPg, which is located at the 5' end of the viral genome, serves as a primer for synthesis of the nascent viral RNA (Nomoto et al. 1977; Virgin-Slane et al. 2012). And it has been speculated that the 14 K protein, which can bind to membranes via its central hydrophobic domain, riveting the replication apparatus onto the endoplasmic reticulum membrane, may be involved in the in vivo accumulation of the viral genome (Schaad et al. 1997). P3 is a further important protein that influences viral RNA accumulation, whereas the P2 protein, which is unique to the viruses in the genus *Bymovirus*, plays essential roles in the transmission of the virus by *Polymyxa graminis* and in the formation of membrane compartments associated with WYMV genome replication (Sun et al. 2014; Li et al. 2017; Xie et al. 2019). In this study, we analyzed the core structural features of the 3' UTR in the regulation of WYMV RNA1 replication, identified the sites to which the Nib protein binds, and determined the regulatory effects of the VPg, P3, and 14 K proteins on Nib protein activity.

Results

WYMV Nib recognizes the WYMV RNA1 3' UTR and catalyzes the synthesis of antisense RNA chains

The WYMV Nib protein has RdRp characteristics and is involved in viral replication. Following prokaryotic expression, we purified the MBP-Nib fusion protein (Fig. 1a). And selected three WYMV RNA1 fragments for in vitro replication. The results revealed that the MBP-Nib protein can specifically recognize the 3' UTR of WYMV RNA1 and catalyze the synthesis of its corresponding complementary strand (Fig. 1b). However, it was unable to catalyze the complementary strand synthesis of the WYMV RNA1 5' UTR and intermediate (Fig. 1b). Moreover, the MBP protein is unable to independently catalyze synthesis of the complementary strand of the WYMV RNA1 3' UTR (Fig. 1b).

To further validate the specificity of the WYMV Nib protein, other WYMV proteins associated with RNA accumulation in the virus involving 14 K, P3, and VPg, and the RdRp of the tobacco bushy top virus (TBTv) (Lu et al. 2017) were selected to verify its specific recognition of the WYMV RNA1 3' UTR. Having purified the MBP-VPg, MBP-14 K, and MBP-P3 fusion proteins following prokaryotic expression (Fig. 1a), we found that the RdRp

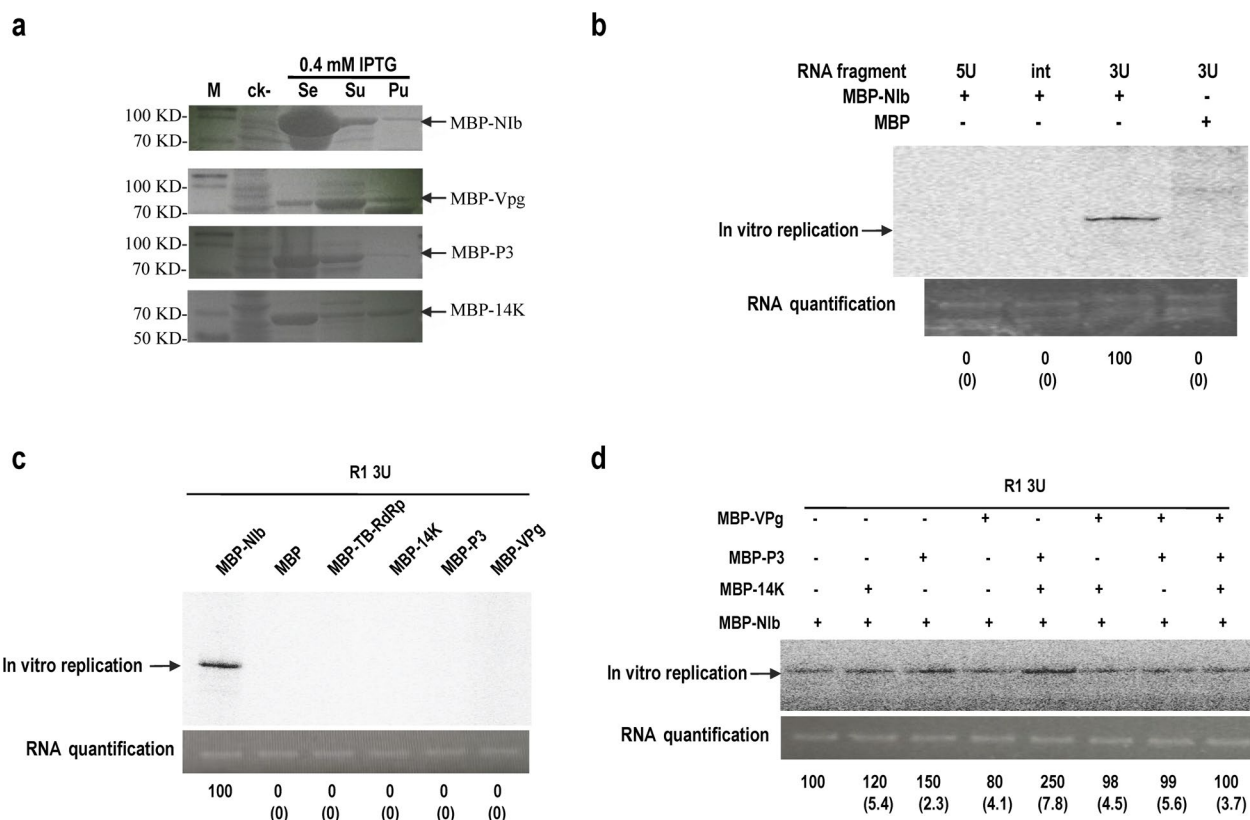


Fig. 1 In vitro transcription of RNA1 by Nib and different proteins of the wheat yellow mosaic virus. **a** SDS-Page gel image for Nib, VPg, P3 and 14 K. M, Protein marker; mock, Without the induction of IPTG; Se, Sediment; Su, Supernatant; Pu, Purified substance; MBP, maltose-binding protein; Nib, Nib protein of WYMV; 14 K, 14 K protein of WYMV; P3, P3 protein of WYMV; VPg, VPg protein of WYMV. **b** In vitro transcription of RNA1 by Nib of the wheat yellow mosaic virus. 5U is 160 nt, int is 160 nt, 3U is 258 nt. **c** Activity of different proteins encoded by WYMV in the in vitro transcription system. TB-RdRp, TBTV RNA-dependent RNA polymerase. **d** Synergistic regulatory effect of different proteins encoded by WYMV on Nib protein activity in the in vitro transcription system. The numbers under the RNA quantification indicate the RNA-level of the complementary strand synthesized by MBP-Nib, and the numbers in brackets indicate the STEV

of TBTV is unable to recognize and catalyze the synthesis of the complementary strand of the WYMV RNA1 3' UTR (Fig. 1c), and that the 14 K, P3, and VPg proteins of WYMV are unable to independently catalyze the synthesis of the 3' UTR complementary strand of WYMV RNA1 (Fig. 1c). Thus, these findings tend to indicate that the WYMV Nib protein can specifically recognize and catalyze the synthesis of the 3' UTR complementary strand of WYMV RNA1.

Further analysis, conducted to assess the regulatory effects of 14 K, P3, and VPg proteins on the RdRp activity of Nib, revealed that in the presence of the 14 K and P3 proteins, the RdRp activities of Nib were enhanced by 1.2- and 1.5-fold, respectively, whereas in the presence of the VPg protein, the efficiency of RdRp activity of Nib was reduced to 80% that of the wild type (Fig. 1d). Subsequently, we examined the regulatory effects of 14 K, P3, and VPg on the RdRp activity of Nib using the respective pairs of these proteins. The results accordingly revealed

that in the presence of the 14 K and P3 proteins, the RdRp activity of Nib was enhanced by 2.5-fold, whereas neither the 14 K and VPg nor P3 and VPg combinations had any significant effect on the RdRp activity of Nib (Fig. 1d). Similarly, the combination of all three of these proteins had no appreciable effects on the RdRp activity of Nib (Fig. 1d).

Core structure of the WYMV RNA1 3' UTR influences replication efficiency

To identify the sites of interaction between the WYMV RNA1 3' UTR and Nib protein, we assessed structural changes in the RNA1 3' UTR in the presence or absence of the Nib protein using an in-line probing assay (Fig. 2a). The end of the RNA1 3' UTR contains five hairpins (H1–H5), as indicated by the in-line cleavage patterns (Fig. 2). In the presence of the Nib protein, the ⁷⁶²⁴UU in the connecting sequence between H1 and H2 and ⁷⁵⁷¹UU in the H4 loop was found to be characterized by

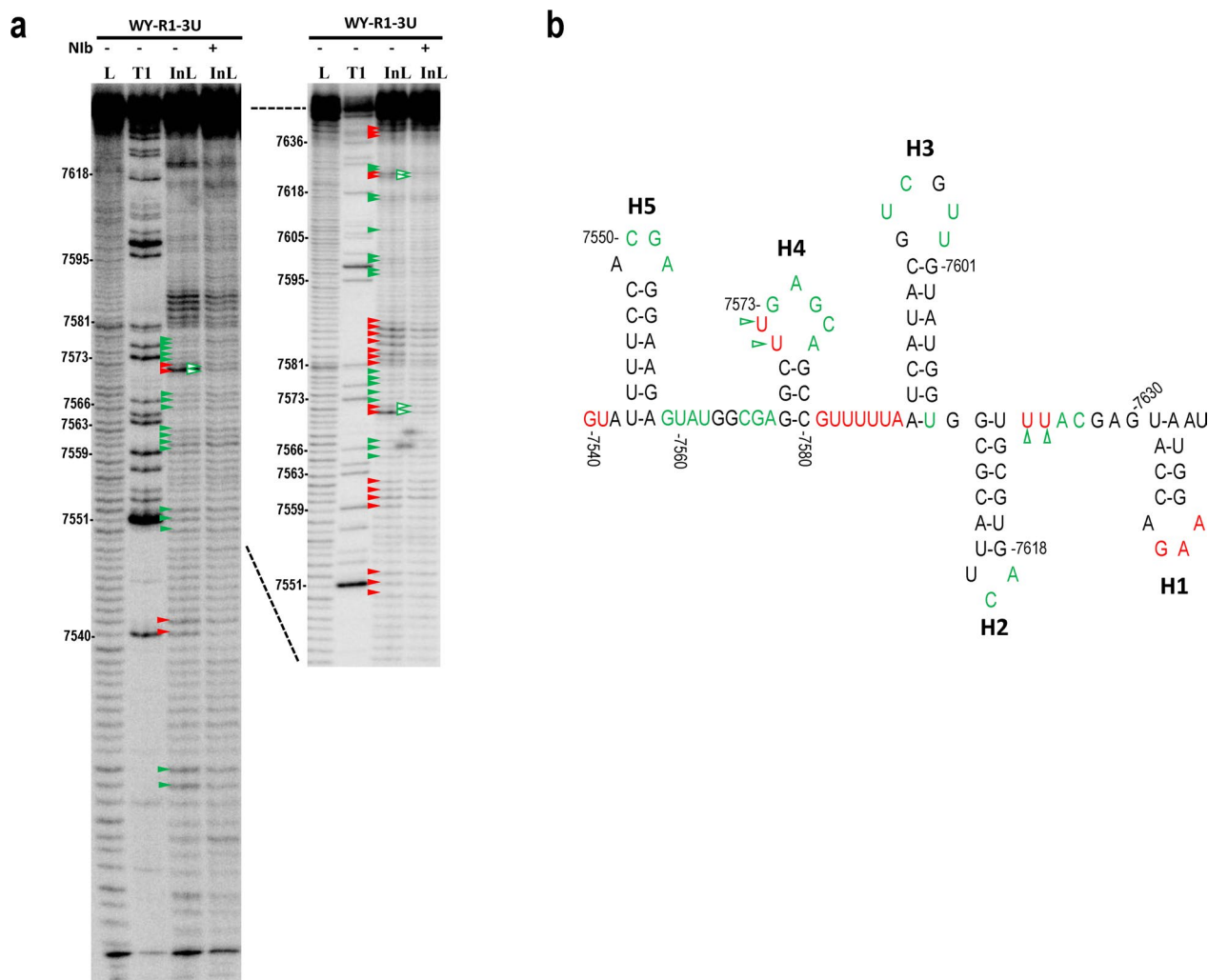


Fig. 2 Structural probing of the 3' UTR of WYMV RNA1 in the presence or absence of the Nib protein. **a** In-line probing of the WYMV RNA1 3' UTR in the presence or absence of the Nib protein. L, ladder generated from treatment with NaOH, which cleaves at arbitrary nucleotides; T1, ladder generated from fragment denaturation and treatment with RNase T1, which cleaves at guanylates. InL: in-line cleavage products, which cleave bases at single-strand status. Base numbering is shown on the left hand side of the panel. Red and green solid triangles indicate strongly and weakly marked cleavage sites in the RNA1 3' UTR, respectively. Green hollow triangles denote the weaker cleavage sites within the RNA1 3' UTR in the presence of the Nib protein versus its absence. **b** RNA structure of the WYMV RNA1 3' UTR in the presence or absence of the Nib protein. Black, green, and red nucleotides, respectively, indicate none or inapparent, marked, and strongly marked cleavage based on the in-line probing pattern. Green and red nucleotides indicate single-strand characteristics. Green hollow triangles denote the weaker cleavage sites within the RNA1 3' UTR in the presence of the Nib protein versus its absence. H1, hairpin 1; H2, hairpin 2; H3, hairpin 3; H4, hairpin 4; H5, hairpin 5

reduced in-line cleavage, which implies newly formed base pairing in response to the presence of the Nib protein (Fig. 2). To map the sites of interaction between the RNA1 3' UTR and Nib protein, we examined the in vitro replication between 3' UTR (or mutants thereof) and Nib (Fig. 3a). The findings revealed that compared with the wild-type RNA1 3' UTR, ML4 and M7624 are unable to catalyze the synthesis of the corresponding antisense strand. Similarly, mutations in the stem of H4 (MS4) also reduced the replication efficiency to 30% of the wild type

(Fig. 3b). These findings imply that ⁷⁶²⁴UU and ⁷⁵⁷¹UU may both serve as sites for interaction with the Nib protein and ensure replication, it is necessary for these sites to coexist.

Mutagenesis was performed to test the effect of H1, H2, H3, and H5 of the 3' UTR on the complementary strand synthesized by MBP-Nib (Fig. 3a). When using the 3' UTR with mutations on the H1 hairpin stem (MS1) or loop (ML1) as a template, the complementary strand synthesized by MBP-Nib decreased to 90% or

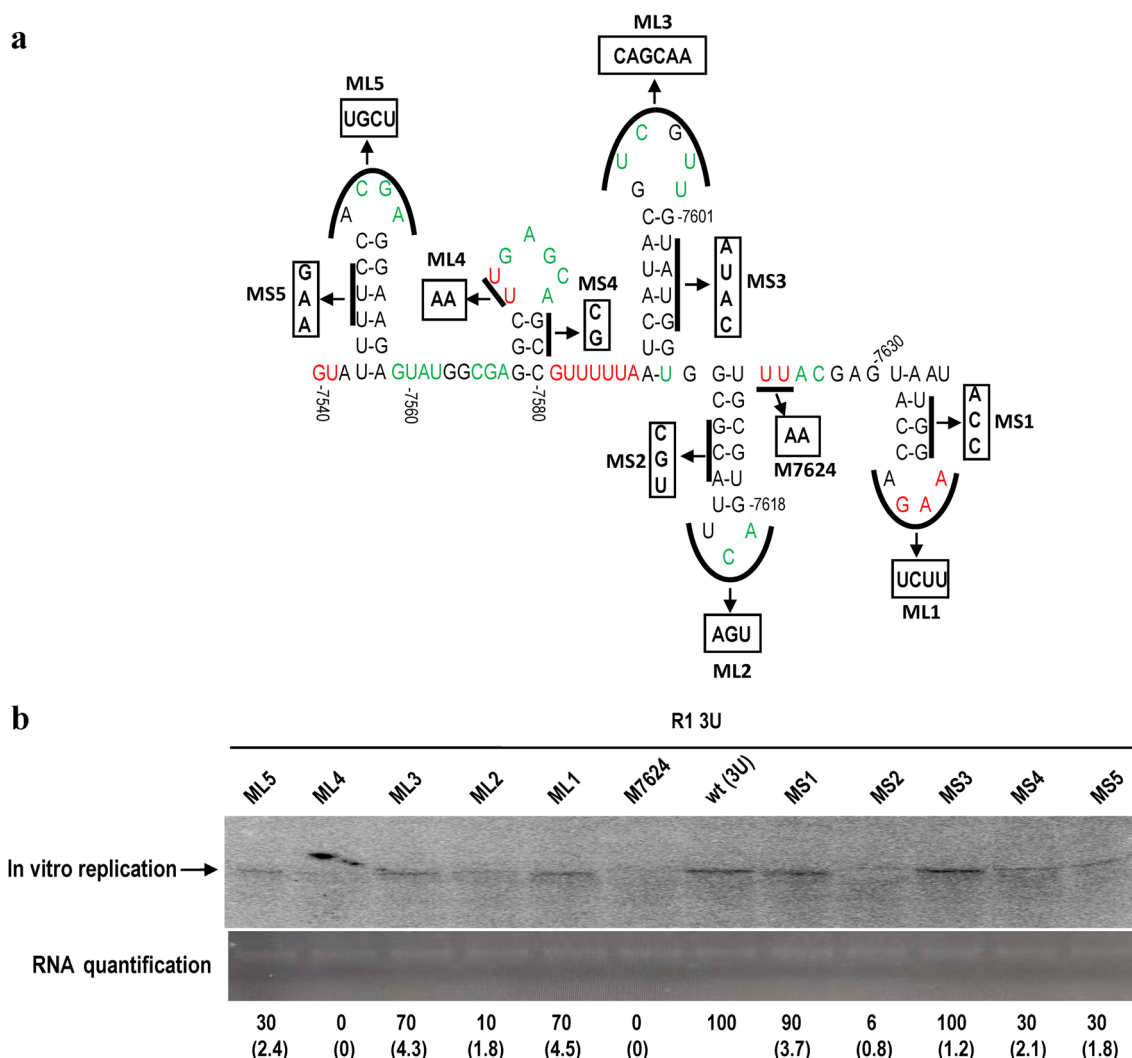


Fig. 3 Core cis-elements within the RNA1 3' UTR involved in the in vitro transcription system. **a** Mutations within the RNA1 3' UTR. **b** In vitro transcription of mutant of 3' UTRs by Nib. The numbers under the RNA quantification indicate the RNA-level of the complementary strand synthesized by MBP-Nib, and the numbers in brackets indicate the STEV

70% of the level when using wt 3' UTR (Fig. 3b). When H2 hairpin of the 3' UTR was mutated on both the stem (MS2) and loop (ML2), the MBP-Nib lost its ability to use these templates to synthesize the complementary strands (Fig. 3b). Whereas when using the 3' UTR harboring mutations in the H3 hairpin stem (MS3) as a template, we detected no evident changes in the efficiency of complementary strand synthesis by MBP-Nib. However, when using the 3' UTR with mutations in the H3 loop (ML3) as a template, the complementary strand synthesized by MBP-Nib was found to be reduced to 70% of the level obtained when using the wild-type 3' UTR (Fig. 3b). Finally, when using the 3' UTR with mutations in both the stem and loop of H5 (MS5 and ML5), synthesis of the complementary strand by MBP-Nib declined to 30%

of the level obtained when using the wild-type 3' UTR (Fig. 3b). These findings thus indicate that mutations in H2 and H5 have a significant effect on the synthesis of the complementary strand by MBP-Nib, which could be associated with changes in the overall structure of the 3' end of RNA1 caused by mutations in H2 and H5, leading to an attenuation of Nib protein binding.

Discussion

Obtaining a purified and active replicase enzyme represents a key step in studying the regulation of viral replication. This can be facilitated by using either virus-infected cells or heterologous expression systems (Hayes and Buck 1990; Hong and Hunt 1996; Kao and Sun 1996; Li et al. 1998; Rajendran et al. 2002). Compared with the

replicase purified from virus-infected cells, which has typically undergone post-translational protein modifications, such as phosphorylation, glycosylation, and ubiquitination, the purified replicase protein obtained using heterologous expression systems, such as *E. coli*, has higher purity. Accordingly, in the present study, we obtained the RdRp protein (N1b protein) from WYMV via prokaryotic expression. This protein was established to have catalytic activity and specificity for RNA recognition (Fig. 1). Among the other WYMV proteins associated with viral accumulation in vivo (Li and Shirako 2015; Zhang et al. 2019a, b), we found that the VPg, 14 K, and P3 proteins are unable to independently catalyze virus genome replication in vitro (Fig. 1c), which is consistent with previous findings (Geng et al. 2019b). However, in the presence of N1b, we found that a combination of the 14 K and P3 proteins enhanced the replicative activity of the N1b protein in vitro (Fig. 1d), thus indicating that these two proteins may form a replication complex with N1b, thereby altering the original conformation of N1b protein, facilitating its bind to the 3' UTR, and potentially determining virus accumulation in vivo. Contrastingly, we found that the VPg protein had an inhibitory effect on replication (Fig. 1d), which could indicate that the primary role of this protein is associated with transcription from a negative to a positive sense. Among picornaviruses, VPg, located at the 5' end, serves as a primer for the synthesis of nascent viral RNA and can be released from viral RNA via the "unlinkase" activity of the TDP2 enzyme (Nomoto et al. 1977; Virgen-Slane et al. 2012). In the present study, we found that transcription of the negative-sense strand from the positive sense could be completed in the absence of VPg. However, given that the transcription of WYMV from a negative to a positive sense has yet to be established, the specific mechanisms of action of the VPg protein during replication remain unclear. Consequently, in further studies, we will seek to establish a transcriptional system for WYMV from the negative to the positive sense, which will serve as a basis for subsequent research.

Wheat yellow mosaic disease is among the most economically important diseases in East Asia, particularly China. It was first reported in the 1970s, has occurred in large numbers, and gradually expanded to Shandong, Zhejiang, Jiangsu, Henan, Hubei, Shanxi, and other provinces (Tao et al. 1980; Wang et al. 1980; Yu et al. 1986). The management of yellow mosaic disease in wheat is primarily dependent on the natural resistance of wheat and genetically modified wheat varieties. Research conducted to date on the translational regulatory mechanism of WYMV has revealed the presence of IRES elements in its 5' UTR and the synergistic

enhancement of IRES activity by 3' UTR (Geng et al. 2020, 2024). However, the independent regulatory mechanisms of WYMV replication have yet to be sufficiently established. In this study, we focused on WYMV RNA1 and found that the purified MBP-N1b protein had higher specificity for the 3' UTR of RNA1 than for other fragments of RNA1 (Fig. 1a), which has also been shown in studies on other viruses (Hong and Hunt 1996; Nagy and Pogany 2000; Rajendran et al. 2002; Yuan et al. 2010; Lu et al. 2017). The 3' end of RNA contains a 'core promoter region' with diverse structural features that interact with RdRp. Some of these features are short sequences without obvious high-level structures, whereas others are elements with distinct structural characteristics, including stem ring structures, pseudo-nodes, and tRNA-like structures (Buck 1996; Dreher 1999; Turner and Buck 1999). In addition to the core promoter region, other sequences or structures located within the 3' end region of the template RNA have been established to be involved in regulating replication, playing either an enhancing or attenuating role (Kim and Makino 1995; Pogany et al. 2003; Zhang et al. 2004). In this study, we identified five hairpin (H1–H5) structures at the end of the RNA1 3' UTR (Fig. 2), and on the basis of an analysis of in-line cleavage patterns, we speculated that the ⁷⁶²⁴UU and ⁷⁵⁷¹UU sequences may serve as binding sites for N1b. However, there are also other possibilities, such as the presence of N1b, which may promote changes in the overall structure of the WYMV RNA1 3' UTR, resulting in the closure of ⁷⁶²⁴UU and ⁷⁵⁷¹UU, leading to a reduction in cleavage. However, regardless of whether ⁷⁶²⁴UU and ⁷⁵⁷¹UU are binding sites for N1b, their importance is self-evident. Mutations at either site were found to inhibit complementary strand synthesis, thereby influencing viral replication (Fig. 3b). Moreover, H2 and H5 were identified as being important for RNA replication (Fig. 3b), as evidenced by our observations indicating that mutations in H2 and H5 may lead to changes in the terminal structure of the RNA1 3' UTR, resulting in a weakening of binding to the N1b protein. Collectively, our findings in this study enabled us to elucidate the core replication regulatory elements of RNA1 replication. Although these results were obtained in vitro, during our prediction of the full-length structure of WYMV RNA1, we found that the structure at the 3' UTR end exists independently. These findings will provide a basis for further research on the regulation of WYMV replication in vivo and will also contribute to the identification of antiviral targets and provide a theoretical basis for the prevention and control of WYMV-caused crop diseases.

Conclusions

In this study, in which we sought to characterize the core structural features of the 3' UTR-regulated replication of WYMV RNA1 in vitro, we identified the sites to which the Nib protein binds and determined the regulatory effects of the VPg, P3, and 14 K proteins on Nib protein activity. We identified five hairpin (H1–H5) structures at the end of the RNA1 3' UTR and established ⁷⁶²⁴UU and ⁷⁵⁷¹UU as putative sites for interaction with the Nib protein, the simultaneously coexistence of which is necessary to ensure replication in vitro. Moreover, H2 and H5 were identified as key hairpin structures for RNA replication in vitro, with mutations in H2 and H5 potentially leading to changes in the terminal structure of the RNA1 3' UTR, resulting in a weakening of the binding to Nib protein. We believe that our characterization of the core replication regulatory elements of RNA1 will serve as a basis for the identification of antiviral targets and provide a theoretical basis for the prevention and control of WYMV-caused crop diseases.

Material and methods

Preparation of DNA fragments

DNA fragments were amplified via PCR to be the template for making corresponding in vitro transcripts, which were used for in-line probing and in vitro replication. Detailed information was shown in Additional file 1: Table S1.

Prokaryotic expression and purification of WYMV Nib, VPg, 14 K and P3

The coding sequences of WYMV Nib, VPg, 14 K and P3 were amplified by PCR and inserted into the pMAL-C2X (NEB) vector through the cleavage sites of the restriction enzymes *Bam*HI and *Sal*I. The positive plasmid was transformed into *E. coli* strain Rosetta. Nib, VPg, 14 K and P3 proteins were expressed under the induction of 0.5 M IPTG at 37 °C for 5 h. The proteins fused with MBP were purified using amylose resin (NEB E8021S) by affinity column chromatography according to the manufacturer's instructions.

The purified WYMV Nib, VPg, 14 K and P3 were used in the following In-line probing and in vitro replication.

In vitro transcription with T7 RNA Polymerase

With the plasmid as template, PCR was performed to amplify different PCR fragments corresponding 3' UTR and their mutations of pUWR1-1. Detailed information for primers and corresponding fragments were listed in Additional file 1: Table S1. Purified PCR products were used to perform in vitro transcription with T7 RNA

polymerase (NEB #M0251S). The target RNAs were separated through 1.5% agarose gel electrophoresis and purified by glass wool.

In-line probing

In-line structure probing was performed as previously described (Geng et al. 2020). The basic principle of this technology is to utilize the unique intramolecular ester transfer reaction of RNA. When the base is unpaired, its 2-position hydroxyl group can rotate freely, resulting in the breakage of the RNA chain at that base; By 8% polyacrylamide gel electrophoresis (8 M urea), the breaking position of RNA can be located, thereby clarifying the single and double-stranded state of RNA chains. Briefly, RNA fragments of the WYMV RNA1 partial 3' UTR (nucleotides 7500–7644) were end-labelled with [γ -³²P] ATP and denatured at 75°C, then slowly cooled to 25°C. RNA was incubated at 25°C in 50 mM Tris–HCl [pH 8.5] and 20 mM MgCl₂ for 14 h. To identify potential RNA–protein interaction, unlabeled protein were co-incubated with isotope-labeled RNA fragments. Samples were separated by 8% polyacrylamide gel electrophoresis (8 M urea) alongside a hydroxide-generated RNA cleavage ladder and RNase T1 digestion product on labelled RNA fragments. Then, the gels were dried and exposed to a phosphorimager screen, followed by detection with the Typhoon FLA-7000 (GE Healthcare). At least two independent in-line probing assays were performed for each fragment.

In vitro replication

The 50 μ L reaction systems consist of 1 μ g of RNA templates, 1 M Tris–Cl (pH 8.2) 5 μ L, 1 M MgCl₂ 0.5 μ L, 1 M DTT 0.5 μ L, 1 M KCl 5 μ L, 10 mg/mL yeast tRNA 1.75 μ L, 20 mM ATP 2.5 μ L, 20 mM GTP 2.5 μ L, 20 mM CTP 2.5 μ L, 1 mM UTP 0.5 μ L, α -³²P-UTP 0.5 μ L, 12.5 μ g of tested protein and ddH₂O. In vitro replication reaction was performed at 20 °C for 1.5 h. After the reaction, 70 μ L ddH₂O and 120 μ L of phenol/chloroform were added followed by centrifugation at 13,000 rpm. The supernatant was precipitated by adding 2.4 times the volume of NH₄Ac/isopropanol (5 M NH₄Ac: isopropanol=1: 5) and placed at –80 °C for at least 2 h. The precipitates were resuspended using 10 μ L RNA loading buffer and separated in 5% PAGE gel containing 8 M urea with 1500 mA for 1.5 h. Then, the gel was dried and exposed to a phosphorimager screen, followed by detection with the Typhoon FLA-7000 (GE Healthcare). At least three independent in vitro replication assays were performed for each construct. The RNA-level results of the complementary strand synthesized by MBP-Nib in all figures have been quantified using ImageJ software.

Supplementary Information

The online version contains supplementary material available at <https://doi.org/10.1186/s42483-024-00300-6>.

Additional file 1: Table S1 The primers used in this experiment.

Acknowledgements

We are grateful to Prof. Chenggui Han (China Agricultural University) for providing the plasmid pUWR1-1.

Author contributions

GG and YX designed experiments. GG performed the experiments and analyzed the data. ML performed analyzed the data. GG wrote the manuscript, YX revised the manuscript. All authors read and approved the final manuscript.

Funding

Shandong Province Natural Sciences Foundation of China (ZR2021QC008); National Natural Science Foundation of China (32100132, 31872638, 32370174); Science and Technology Support Plan for Youth Innovation of Colleges and Universities of Shandong Province of China (2022KJ119); Young Talent of Lifting engineering for Science and Technology in Shandong (SDAST2024QT085).

Availability of data and materials

Not applicable.

Declarations

Ethics approval and consent to participate

Not applicable.

Consent for publication

Not applicable.

Competing interests

The authors declare that they have no competing interests.

Received: 12 August 2024 Accepted: 16 December 2024

Published online: 24 February 2025

References

- Buck KW. Comparison of the replication of positive-stranded RNA viruses of plants and animals. *Adv Virus Res.* 1996;47:159–251. [https://doi.org/10.1016/S0065-3527\(08\)60736-8](https://doi.org/10.1016/S0065-3527(08)60736-8).
- Chen J, Sohn A, Chen JP, Lei J, Cheng Y, Schulze S, et al. Molecular comparisons amongst wheat bymovirus isolates from Asia North America and Europe. *Plant Pathol.* 1999;48:642–7. <https://doi.org/10.1046/j.1365-3059.1999.00392.x>.
- Dreher TW. Functions of the 3′-untranslated regions of positive strand RNA viral genomes. *Annu Rev Phytopathol.* 1999;37:151–74. <https://doi.org/10.1146/annurev.phyto.37.1.151>.
- Ferrer-Orta C, Arias A, Escarmis C, Verdaguer N. A comparison of viral RNA-dependent RNA polymerases. *Curr Opin Struct Biol.* 2006;16:27–34. <https://doi.org/10.1016/j.sbi.2005.12.002>.
- Geng G, Yu C, Wang D, Gu K, Shi K, Li X, et al. Evolutional analysis of two new isolates of Wheat yellow mosaic virus from Shandong Province China. *Acta Phytopathol Sin.* 2017;49:348–56. <https://doi.org/10.13926/j.cnki.apps.000104> (in Chinese).
- Geng G, Yu C, Li X, Yuan X. Variable 3′ polyadenylation of Wheat yellow mosaic virus and its novel effects on translation and replication. *Virology.* 2019a;16:1–8. <https://doi.org/10.1186/s12985-019-1130-z>.
- Geng G, Yu C, Li X, Yuan X. In vitro transcription system based on Nib of wheat yellow mosaic virus. *Acta Phytopathol Sin.* 2019b;49:212–8. <https://doi.org/10.13926/j.cnki.apps.000370> (in Chinese).
- Geng G, Yu C, Li X, Yuan X. A unique internal ribosome entry site representing a dynamic equilibrium state of RNA tertiary structure in the 5′UTR of wheat yellow mosaic virus RNA1. *Nucleic Acids Res.* 2020;48:390–404. <https://doi.org/10.1093/nar/gkz1073>.
- Geng G, Yu C, Yuan X. Variable eIF4E-binding sites and their synergistic effect on cap-independent translation in a novel IRES of wheat yellow mosaic virus RNA2 isolates. *Int J Biol Macromol.* 2024;254: 128062. <https://doi.org/10.1016/j.ijbiomac.2023.128062>.
- Hariri D, Courtillot M, Zaoui P, Lapiere H. Multiplication of Soilborne wheat mosaic virus (SBWMV) in wheat roots infected by a soil carrying SBWMV and wheat yellow mosaic virus. *Agronomie.* 1987;7:789–96. <https://doi.org/10.1051/agro:19871005>.
- Hayes RJ, Buck KW. Complete replication of a eukaryotic virus RNA in vitro by a purified RNA-dependent RNA polymerase. *Cell.* 1990;63:363–8. [https://doi.org/10.1016/0092-8674\(90\)90169-f](https://doi.org/10.1016/0092-8674(90)90169-f).
- Hong Y, Hunt AG. RNA polymerase activity catalyzed by a potyvirus-encoded RNA-dependent RNA polymerase. *Virology.* 1996;226:146–51. <https://doi.org/10.1006/viro.1996.0639>.
- Kao CC, Sun JH. Initiation of minus-strand RNA synthesis by the Brome mosaic virus RNA-dependent RNA polymerase: use of oligoribonucleotide primers. *J Virol.* 1996;70:6826–30. <https://doi.org/10.1007/BF02848694>.
- Khromykh AA, Meka H, Guyatt KJ, Westaway EG. Essential role of cyclization sequences in flavivirus RNA replication. *J Virol.* 2001;75:6719–28. <https://doi.org/10.1128/JVI.75.14.6719-6728.2001>.
- Kim KH, Hemenway CL. Long-distance RNA-RNA interactions and conserved sequence elements affect potato virus X plus-strand RNA accumulation. *RNA.* 1999;5:636–45. <https://doi.org/10.1017/S1355838299982006>.
- Kim YN, Makino S. Characterization of a murine coronavirus defective interfering RNA internal cis-acting replication signal. *J Virol.* 1995;69:4963–71. [https://doi.org/10.1016/0166-0934\(95\)00037-U](https://doi.org/10.1016/0166-0934(95)00037-U).
- Koonin EV, Gorbalenya AE, Chumakov KM. Tentative identification of RNA-dependent RNA polymerases of dsRNA viruses and their relationship to positive strand RNA viral polymerases. *Febs Lett.* 1989;252:42–6. [https://doi.org/10.1016/0014-5793\(89\)80886-5](https://doi.org/10.1016/0014-5793(89)80886-5).
- Lewandowski DJ, Dawson WO. Functions of the 126- and 183-kDa proteins of tobacco mosaic virus. *Virology.* 2000;271:90–8. <https://doi.org/10.1006/viro.2000.0313>.
- Li H, Shirako Y. Association of VPg and eIF4E in the host tropism at the cellular level of Barley yellow mosaic virus and wheat yellow mosaic virus in the genus Bymovirus. *Virology.* 2015;476:159–67. <https://doi.org/10.1016/j.virol.2014.12.010>.
- Li YI, Cheng YM, Huang YL, Tsai CH, Hsu YH, Meng MH. Identification and characterization of the escherichia coli-expressed rna-dependent rna polymerase of bamboo mosaic virus. *J Virol.* 1998;72:10093–9. <https://doi.org/10.1016/j.jacc.2014.07.851>.
- Li D, Yan L, Su N, Han C, Hou Z, Yu J, et al. The nucleotide sequence of a Chinese isolate of wheat yellow mosaic virus and its comparison with a Japanese isolate. *Arch Virol.* 1999;144:2201–6. <https://doi.org/10.1007/s007050050633>.
- Li L, Andika IB, Xu Y, Zhang Y, Xin X, Hu L, et al. Differential characteristics of viral siRNAs between leaves and roots of wheat plants naturally infected with wheat yellow mosaic virus, a soil-borne virus. *Front Microbiol.* 2017;8:1802. <https://doi.org/10.3389/fmicb.2017.01802>.
- Lin M, Ruan Y. A study on wheat yellow mosaic virus. *Acta Phytopathol Sin.* 1986;2:11–6. <https://doi.org/10.13926/j.cnki.apps.1986.02.002> (in Chinese).
- Lu X, Yu C, Wang G, Wang D, Geng G, Liu S, et al. In vitro replication system mediated by RNA-dependent RNA polymerase (RdRp) in Tobacco bushy top virus. *Acta Phytopathol Sin.* 2017;47:790–6. <https://doi.org/10.13926/j.cnki.apps.000116> (in Chinese).
- Miller WA, White KA. Long-distance RNA-RNA interactions in plant virus gene expression and replication. *Annu Rev Phytopathol.* 2006;44:447–67. <https://doi.org/10.1146/annurev.phyto.44.070505.143353>.
- Nagy PD, Pogany J. Partial purification and characterization of cucumber necrosis virus and Tomato bushy stunt virus RNA-dependent RNA polymerases: similarities and differences in template usage between tombusvirus and carmovirus RNA-dependent RNA polymerases. *Virology.* 2000;276:279–88. <https://doi.org/10.1006/viro.2000.0577>.
- Namba S, Kashiwazaki S, Lu X, Tamura M, Tsuchizaki T. Complete nucleotide sequence of wheat yellow mosaic by movirus genomic RNAs. *Arch Virol.* 1998;143:631–43. <https://doi.org/10.1007/s007050050319>.

- Nomoto A, Detjen B, Pozzatti R, Wimmer E. The location of the poliogenome protein in viral RNAs and its implication for RNA synthesis. *Nature*. 1977;268:208–13. <https://doi.org/10.1038/268208a0>.
- Pogany J, Fabian MR, White KA, Nagy PD. A replication silencer element in a plus-strand RNA virus. *EMBO J*. 2003;22:5602–11. <https://doi.org/10.1093/emboj/cdg523>.
- Rajendran KS, Pogany J, Nagy PD. Comparison of Turnip crinkle virus RNA-dependent RNA polymerase preparations expressed in *Escherichia coli* or derived from infected plants. *J Virol*. 2002;76:1707–17. <https://doi.org/10.1128/jvi.76.4.1707-1717.2002>.
- Sanford TJ, Mears HV, Fajardo T, Locker N, Sweeney TR. Circularization of flavivirus genomic RNA inhibits de novo translation initiation. *Nucleic Acids Res*. 2019;47:18. <https://doi.org/10.1093/nar/gkz686>.
- Schaad MC, Jensen PE, Carrington JC. Formation of plant RNA virus replication-complexes on membranes: role of an endoplasmic reticulum-targeted viral protein. *EMBO J*. 1997;16:4049–59. <https://doi.org/10.1093/emboj/16.13.4049>.
- Sun L, Andika IB, Shen J, Yang D, Chen J. The P2 of Wheat yellow mosaic virus rearranges the endoplasmic reticulum and recruits other viral proteins into replication-associated inclusion bodies. *Mol Plant Pathol*. 2014;15:466–78. <https://doi.org/10.1111/mpp.12109>.
- Tao J, Qin J, Xiao J, Shen Y, Li T, Xie Y, et al. Studies on the soil-borne yellow mosaic virus of wheat in Sichuan. *Acta Phytopathol Sin*. 1980;10:5–25. <https://doi.org/10.13926/j.cnki.apps.1980.01.002> (in Chinese).
- Turner RL, Buck KW. Mutational analysis of cis-acting sequences in the 3′- and 5′-untranslated regions of RNA2 of red clover necrotic mosaic virus. *Virology*. 1999;253:115–24. <https://doi.org/10.1006/viro.1998.9495>.
- van Dijk AA, Makeyev EV, Bamford DH. Initiation of viral RNA-dependent RNA polymerization. *J Gen Virol*. 2004;85:1077–93. <https://doi.org/10.1099/vir.0.19731-0>.
- Virgen-Slane R, Rozovics JM, Fitzgerald KD, Ngo T, Chou W, van der Hedenvan Noort GJ, et al. An RNA virus hijacks anincognito function of a DNA repair enzyme. *Proc Natl Acad Sci USA*. 2012;109:14634–9. <https://doi.org/10.1073/pnas.1208096109>.
- Wang N, Liu G, Lu X. Preliminary study on wheat spindle streak mosaic virus place in China. *Sichuan Agric Sci Technol*. 1980;1:34–5 (in Chinese).
- Wang X, Liu Y, Han C, Wu Y, Zhao Z. Present situation and development strategies for the research and control of wheat viral diseases. *Plant Prot*. 2010;36:13–9. <https://doi.org/10.3969/j.issn.0529-1542.2010.03.004> (in Chinese).
- Xie L, Song X, Liao Z, Wu B, Yang J, Zhang H, et al. Endoplasmic reticulum remodeling induced by Wheat yellow mosaic virus infection studied by transmission electron microscopy. *Micron*. 2019;120:80–90. <https://doi.org/10.1016/j.micron.2019.01.007>.
- Yu S, Chen Z, Xu L, Zhang R, Wang M, Luo R. Wheat yellow mosaic virus disease in China. *Acta Phytopathol Sin*. 1986;13:217–9. <https://doi.org/10.13802/j.cnki.zwbhxb.1986.04.001> (in Chinese).
- Yu J, Yan L, Su N, Huo Z, Li D, Han C, et al. Analysis of nucleotide sequence of Wheat yellow mosaic virus genomic RNAs. *Sci China Ser C: Life Sci*. 1999;05:108–14.
- Yuan X, Shi K, Meskauskas A, Simon AE. The 3′ end of Turnip Crinkle Virus contains a highly interactive structure including a translational enhancer that is disrupted by binding to the RNA-dependent RNA polymerase. *RNA*. 2009;15:1849–64. <https://doi.org/10.1261/rna.1708709>.
- Yuan X, Shi K, Young M, Simon AE. The terminal loop of a 3′ proximal hairpin plays a critical role in replication and the structure of the 3′ region of Turnip crinkle virus. *Virology*. 2010;402:271–80. <https://doi.org/10.1016/j.virol.2010.03.036>.
- Zhang G, Zhang J, Simon AE. Repression and derepression of minus strand synthesis in a plus-strand RNA virus replicon. *J Virol*. 2004;78:7619–33. <https://doi.org/10.1128/JVI.78.14.7619-7633.2004>.
- Zhang T, Liu P, Zhong K, Zhang F, Xu M, He L, et al. Wheat yellow mosaic virus Nib interacting with host light induced protein (LIP) facilitates its infection through perturbing the abscisic acid pathway in wheat. *Biology*. 2019a;8:80. <https://doi.org/10.3390/biology8040080>.
- Zhang Y, Qi Y, Lu Y, Yang Q, He Y, Li J, et al. Identification and analysis of the pathogenic functional domain of wheat yellow mosaic virus P3 protein. *Acta Agric Univ Zhejiangensis*. 2019b;31:777–83. <https://doi.org/10.3969/j.issn.1004-1524.2019.05.13>(inChinese).